ARTICLE
Journal of Cellular Biochemistry 116:2637–2648 (2015)

Journal of Cellular Biochemistry

Low Dose of IGF-I Increases Cell Size of Skeletal Muscle Satellite Cells via Akt/S6K Signaling Pathway

Chun-qi Gao,[1] Rui Zhi,[1,2] Zhou Yang,[1,3] Hai-chang Li,[4] Hui-chao Yan,[1] and Xiu-qi Wang[1]*

[1]*College of Animal Science, South China Agricultural University/National Engineering Research Center for Breeding Swine Industry/Guangdong Provincial Key Laboratory of Agro-Animal Genomics, Guangzhou, Guangdong province, China*

[2]*Guizhou Agricultural Vocational College, Guiyang, Guizhou, China*

[3]*College of Science and Engineering, Guangxi Open University, Nanning, Guangxi, China*

[4]*Davis Heart & Lung Research Institute, Wexner Medical Center at the Ohio State University, Columbus, Ohio*

ABSTRACT

The objective of this study was to investigate the effect of insulin growth factor-I (IGF-I) on the size of pig skeletal muscle satellite cells (SCs). Using microarray, real-time RT-PCR, radioimmunoassay analysis and western blot, we first showed that supplementation of low-dose of IGF-I in culture medium resulted in enlarged cell size of Lantang SCs, only Akt and S6K were up-regulated at both the mRNA and protein levels among almost all of the mTOR pathway key genes, but had no effect on cell number. To elucidate the signaling mechanisms responsible for regulating cell size under low-dose of IGF-I treatment, we blocked Akt and S6K activity with the specific inhibitors MK2206 and PF4708671, respectively. Both inhibitors caused a decrease in cell size. In addition, MK2206 lowered the protein level of p-Akt (Ser473), p-S6K (Thr389), and p-rpS6 (Ser235/236), whereas PF4708671 lowered the protein level of p-S6K (Thr389) and p-rpS6 (Ser235/236). However, low dose of IGF-I didn't affect the protein level of p-mTOR (Ser2448) and p-mTOR (Ser2481). When both inhibitors were applied simultaneously, the effect was the same as that of the Akt inhibition alone. Taken together, we report for the first time that low-dose of IGF-I treatment increases cell size via Akt/S6K signaling pathway. J. Cell. Biochem. 116: 2637–2648, 2015.

KEY WORDS: IGF-I; SATELLITE CELLS; CELL SIZE; mTOR; AKT; S6K

Insulin-like growth factor-I (IGF-I), a peptide growth hormone with a high sequence similarity to insulin, affects the growth of diverse tissues. In particular, IGF-I serves as an autocrine/paracrine mediator in muscular processes that stimulates both proliferation and differentiation of myoblasts [Duan et al., 2010]. IGF-I plays important roles in various processes that are related to muscle growth, such as muscle regeneration [Ye et al., 2013], and myofiber hypertrophy [Barton et al., 2010].

Mammalian target of rapamycin complex1 (mTORC1) is a serine-threonine kinase that controls cellular processes such as protein synthesis, cell growth, and cell proliferation in response to nutrients (amino acids), growth factors (insulin and IGF-I), cellular energy status (ATP) and mechanical stimulate. The best-defined substrates of mTORC1 are the 70-kDa ribosomal protein S6 kinase (S6K) and eukaryotic translation initiation factor 4E-binding protein 1 (4E-BP1) [Hoeffer and Klann, 2010], both of which are important in regulating protein translation initiation [Hinnebusch, 2012].

The binding of IGF-I to its receptor activates multiple signaling pathways, one of these pathways is the PI3K/Akt/mTORC1 axis [Spangenburg, 2009]. Numerous studies have shown that the mTOR pathway is responsible for cell growth and proliferation response to IGF-I [Zhang et al., 2012; Ge et al., 2013]. However, both cell growth

Chun-qi Gao and Rui Zhi equally contribute to this work.
Conflict of interest: None.

Grant sponsor: National Basic Research Program of China; Grant number: 2012CB124704; Grant sponsor: National 948 Program of China; Grant number: 2011-G35; Grant sponsor: Science and Technology Planning Project of Guangzhou; Grant number: 201300000035.

*Correspondence to: Xiu-Qi Wang, College of Animal Science, South China Agricultural University, Guangzhou, Guangdong 510642, China.
E-mail: xqwang@scau.edu.cn

Manuscript Received: 27 January 2015; Manuscript Accepted: 22 April 2015
Accepted manuscript online in Wiley Online Library (wileyonlinelibrary.com): 29 April 2015
DOI 10.1002/jcb.25212 • © 2015 Wiley Periodicals, Inc.

(mass accumulation: cell size is one of indicators of cell growth) and cell proliferation (cell division: cell number is one of indicators of cell proliferation) contribute to the growth of organs and they are clearly separable processes [Lloyd, 2013]. In Drosophila and mice, Akt and S6K, targets of TOR pathway, have been shown to regulate cell size [Montagne et al., 1999; Condorelli et al., 2002].

In addition, phospholipase D 1 (PLD1) has been shown to act through mTOR/S6K signaling pathway to induce muscle cell enlargement [Jaafar et al., 2013]. Collectively, these data suggest that the mTOR/S6K pathway is critical for promoting cell growth. Nevertheless, 4E-BPs, another target of mTOR pathway, mediates the effects of mTOR to increase cell number but not cell size in mammalian cells [Dowling et al., 2010]. Recently, Cheng et al. [2011] suggested that mTOR is not required for the cell growth in Drosophila. It indicated that the regulation of cell size via IGF-I/mTOR remain poorly understood.

As the resident stem cells, skeletal muscle satellite cells (SCs) are considered to be essential for skeletal muscle regeneration involving in damage repair of muscle [Song et al., 2013]. Our previous results have shown that Lantang pig SCs are more proliferative than Landrace pig SCs, while the cell size of Lantang SCs is significantly smaller than that of Landrace SCs at 72 h after seeding [Wang et al., 2012]. What's more, the trends of cell size and cell number are different. We then hypothesized that IGF-I concentration autocrined by SCs is different between Lantang and Landrace pig and the IGF-I/mTOR pathway may participate in the regulation of cell growth differing from the regulation of cell proliferation. Therefore, Lantang and Landrace SCs are used for investigating the underlying mechanism of IGF-I/mTOR pathway on cell growth.

MATERIALS AND METHODS

CHEMICALS

Anti-Desmin and SABC kit were purchased from Boster Bio-engineerting Co. Ltd (Wuhan, China); Histostain-Plus kit was purchased from Jingmei Biotech Co. Ltd (Shenzhen, China); Recombinant Human IGF-I was purchased from R&D Systems Inc. (Minneapolis, MN). The Akt-specific inhibitor MK2206 was purchased from Selleck Chemicals (Houston, TX), and the S6K-specific inhibitor PF-4708671 was purchased from TOCRIS Bio-science (Bristol, UK). Dimethyl sulfoxide (DMSO) was purchased from Sigma (St. Louis, MO). Anti-Akt, anti-phospho-Akt (Ser473), anti-mTOR, anti-phospho-mTOR (Ser2448), anti-phospho-mTOR (Ser2481), anti-S6K, anti-phospho-S6K (Thr389), anti-rpS6, and anti-phospho-rpS6 (Ser235/236) antibodies were all purchased from Cell Signaling Technology (Beverly, MA). Anti-rabbit IgG and anti-mouse IgG were from Beijing Biosynthesis Biotechnology Co. Ltd (Beijing, China).

CELL CULTURE

The study was conducted with the approval of and in accordance with the directives of the Institutional Animal Care and Use Committee of South China Agricultural University (Guangzhou, China). The SCs were isolated, purified and identified according to the procedures outlined by our research group [Wang et al., 2012]. SCs that were isolated from the longissimus dorsi muscles of newborn Lantang or Landrace pigs were grown and maintained in DMEM/F12 medium containing 10% (v/v) FBS at 37°C in a 5% CO_2 atmosphere. Immunocytochemistry analysis showed that the isolated SCs were positive for the mouse monoclonal antibody against desmin (data not shown).

MICROARRAY ANALYSIS

RNA was isolated from cultured Lantang and Landrace SCs at 72 h after seeding with the Trizol reagent (Invitrogen, Carlsbad, CA) according to manufacturer's instructions. RNA quality was assessed by agarose gel electrophoresis (1%). All of the RNA samples had OD260/OD280 ratios between 1.8 and 2.0. The RNA samples were sent to CapitalBio (Beijing, China) for microarray hybridization. Each RNA sample from different PAM treatments was hybridized to one Roche NimbleGen Porcine Genome Expression Array (Madison, WI). Microarray hybridization and data analysis were performed according to the procedures outlined by Ma et al. [2012]. There were three replicates in Lantang and Landrace SCs.

RADIOIMMUNOASSAY OF IGF-I CONCENTRATION

The culture supernatants of Lantang and Landrace SCs were collected at 72 h after seeding, and IGF-I concentrations were measured by radioimmunoassay using a commercial kit specific to the pig IGF-I (Tianjin Nine Tripods Medical & Bioengineering Co. Ltd., Tianjin, China).

CELL SIZE ANALYSIS

Hematoxylin-eosin (HE) staining. For cell size assessment, SCs from Lantang or Landrace pigs were seeded into 96-well plates at a density of 2×10^3 cells/well. Cells were harvested at 24, 36, 48, 60, 72, 84, and 96 h and rinsed twice with PBS, followed by fixation in 4% paraformaldehyde for 30 min at room temperature. The cells were stained with hematoxylin-eosin (Jingmei Biotech Co. Ltd, Shenzhen, China) and photographed. The pictures were examined using an image processing system (NIS-Elements, Nikon, Japan).

Flow cytometry. SCs were seeded into 6-well plates at a density of 1×10^5 cells/well, and harvested at 36, 48, 60, 72, 84 and 96 h after seeding. To harvest the cells, the plates were washed once with PBS alone and once quickly with PBS/EDTA (2.5 mmol/L), and then incubated at 37°C for 5 min in 1 mL of PBS/EDTA. The cells were gently pipetted off the plates, transferred to 1.5 mL conical tubes, and centrifuged for 5 min at 1,000 rpm. The cells were then washed once in PBS containing 1% FBS, centrifuged for 5 min at 1,000 rpm, resuspended in 0.5 mL of PBS, and fixed by adding 5 mL of 75% ethanol (80% final). Fixed cells were stored at 4°C until analysis. For FACS analysis, 10,000 single cells were collected. The mean FSC-A of the 10,000 single cells was determined as a measure of relative cell size [Rosner et al., 2003].

CELL VIABILITY ASSAY

SCs were seeded into 96-well microtiter plates at a density of 2×10^3 cells/well for cell viability analysis. A total of 20 μL MTT (3-(4, 5-dimethylthiazol-2-yl)-2, 5-diphenyl tetrazolium bromide) solution (Sigma, St. Louis, MO) was added to each well and the plates were incubated for 4 h. The plates were then centrifuged at 1400 g at 25°C

for 15 min. The supernatant was carefully discarded and 150 μL DMSO was added to each well for 10 min at room temperature. The absorbance of the reaction product was measured with a microplate reader at a wavelength of 490 nm.

QUANTITATIVE REAL-TIME POLYMERASE CHAIN REACTION (qRT-PCR)

qRT-PCR was performed using One-Step SYBR Green PCR Mix (Takara, Dalian, China) containing $MgCl_2$, dNTPs, and HotStar Taq polymerase. Primers were designed specifically for each gene using the Primer 5.0 software. Amplification and melting curve analysis were performed on a Stratagene Mx3005P real-time PCR system (Stratagene, La Jolla, CA). Melting curve analysis was conducted to confirm the specificity of each PCR product, and the sizes of products were verified by electrophoresis on ethidium bromide-stained 1.0% agarose gels in Tris acetate-EDTA buffer. Relative mRNA expression level was calculated by $2^{-\triangle Ct}$ ($\triangle Ct = \triangle Ct$ of the target gene $- \triangle Ct$ of the housekeeping gene), with GAPDH as the housekeeping gene. Each sample was analyzed twelve times. The primer sequences (5′ to 3′) were as follows: IGF-I forward: TTC AGT TCG TGT GCG GAG AC, reverse: TGT ACT TCC TTC TGA GCC TTG G; PI3K forward: AAG TGA GAA TGG TCC GAA TG, reverse: TGT CCC CAA CTC CAA GAA T; Akt forward: ACA ACC AGG ACC ACG AGA AG, reverse: GAA ACG GTG CTG CAT GAT CT; TSC1 forward: GGA ACT GGA ATC TCA TCT GG, reverse: TCT TCT GAG CCT CGT ACC TG; mTOR forward: GGT TTG ATT ATG GTC ACT GG, reverse: TGC AAT GAG CTG AGG TAT AA; eIF4E forward: TAC TGT TGA AGA CTT TTG GG, reverse: CAC ATA GGC TCA ATA CCA TC; 4EBP1 forward: AGT GTC GGA ACT CAC CTG T, reverse: TTC TGG CTG GCA TCT GT; S6K forward: TGG AAC TCT TAG GCA CAT CA, reverse: CGA CAC AAT CAG AAC TCA AC; GAPDH forward: GGT CGG AGT GAA CGG ATT TG, reverse: CCT TGA CTG TGC CGT GGA AT.

WESTERN BLOTTING

SCs were washed twice with cold PBS and incubated in a lysis buffer (RIPA, BioTeke, Beijing, China) containing 1 mmol/L protease inhibitor PMSF (Sigma, St. Louis, MO) and phosphatase inhibitors (Sigma, St. Louis, MO) for 20 s on ice, followed by centrifugation at 12,000 g and 4°C for 5 min. The protein concentrations of the supernatants were determined using a BCA Protein Assay Reagent Kit (Thermo Fisher Scientific, Rockford). The protein samples were boiled for 10 min and then subjected to 8–10% SDS gel electrophoresis. The proteins were separated by electrophoresis at 80 V for 20 min and 110 V for 75 min using Tris-glycine running buffer (0.025 mol/L Tris base, 0.192 mol/L glycine, and 0.1% SDS, pH 8.3). Prestained molecular weight markers (Invitrogen, Carlsbad, CA) were used to determine protein size. The proteins were subsequently transferred onto PVDF membranes using a transfer buffer that contained 25 mmol/L Tris base, 192 mmol/L glycine, and 10% methanol (pH 8.1 to 8.3). The membranes were blocked for 1 h in 5% BSA and TBS buffer (20 mmol/L Tris and 500 mmol/L NaCl, pH 7.6) at room temperature. The membranes were then incubated overnight at 4°C with primary antibodies. All antibody dilutions were made in TBST buffer (TBS buffer with 0.05% Tween-20). The membranes were washed 6 times for 5 min each with TBST buffer, followed by incubation for 1 h with horseradish peroxidase-labeled anti-mouse or anti-rabbit IgG (Beijing, China). The proteins were visualized with the ECL-Plus western blotting reagent in a FluorChem M system (Cell Bioscicences, San Leandro, CA). Band density was analyzed by Image J (http://rsb.info.nih.gov/ij/).

STATISTICAL ANALYSIS

Data are expressed as the mean ± SEM. The results were analyzed with Student's *t*-test and One-Way ANOVA using the SAS (version 9.3) software. Differences among groups were determined using Duncan's multiple-range test. The differences between treatments were considered statistically significant when $P < 0.05$.

RESULTS

DIFFERENTIAL IGF-I GENE EXPRESSION IN LANTANG AND LANDRACE SCs

We first examined the gene expression profiles of Lantang and Landrace SCs at 72 h after seeding. The Roche NimbleGen Porcine Genome Expression Array showed that 17,054 transcripts were present in these SCs from two pig breeds (Fig. 1A). At a predefined significance level, 1,727 transcripts were identified to be differentially expressed between the two types of SCs. Compared with the Landrace SCs, 1,258 transcripts in the Lantang SCs were up-regulated and 469 transcripts were down-regulated ($P < 0.05$, FC ≥ 1.5) (Fig. 1A). Microarray found that IGF-I gene expression in Lantang SCs was lower than that in Landrace SCs at 72 h after seeding ($P < 0.05$, FC ≥ 1.5), we further validated IGF-I expression in the SCs by qRT-PCR (Fig. 1B). To confirm the differential expression of IGF-I, we measured the IGF-I concentration in the culture medium of Lantang and Landrace SCs by a radioimmunoassay and found that there was less IGF-I present in the Lantang SCs culture medium than in the Landrace SCs culture medium ($P < 0.05$) (Fig. 1C).

SUPPLEMENTATION OF IGF-I IN LANTANG AND LANDRACE SCs

In order to validate whether the same reaction to the IGF-I between Lantang and Landrace SCs, we proceeded to further evaluate the cellular effects of IGF-I in Lantang and Landrace SCs by exogenously adding increasing doses of IGF-I (0 ng/mL, 10 ng/mL, 25 ng/mL, 50 ng/mL, and 100 ng/mL) to the culture medium. Both types of SCs responded similarly to IGF-I in terms of cell number and size, indicating that IGF-I affected the SCs from the two pig breeds to a similar extent (data not shown). Given that we previously observed different concentrations of extracellular IGF-I between the Lantang and Landrace SCs, to compensate for such a difference, we added exogenous IGF-I to the Lantang SCs culture so that the IGF-I level in the medium would be similar to the level in the Landrace SCs culture medium at 72 h after seeding (Fig. 2A). Based on radioimmunoassay analysis, 7 ng/mL of IGF-I was added to the Lantang SCs culture medium. Similar with results in IGF-I dose response experiment, HE staining and MTT assay showed that low dose of IGF-I increased the cell size (Fig. 2B) but not the cell number of SCs ($P < 0.05$) (Fig 2C).

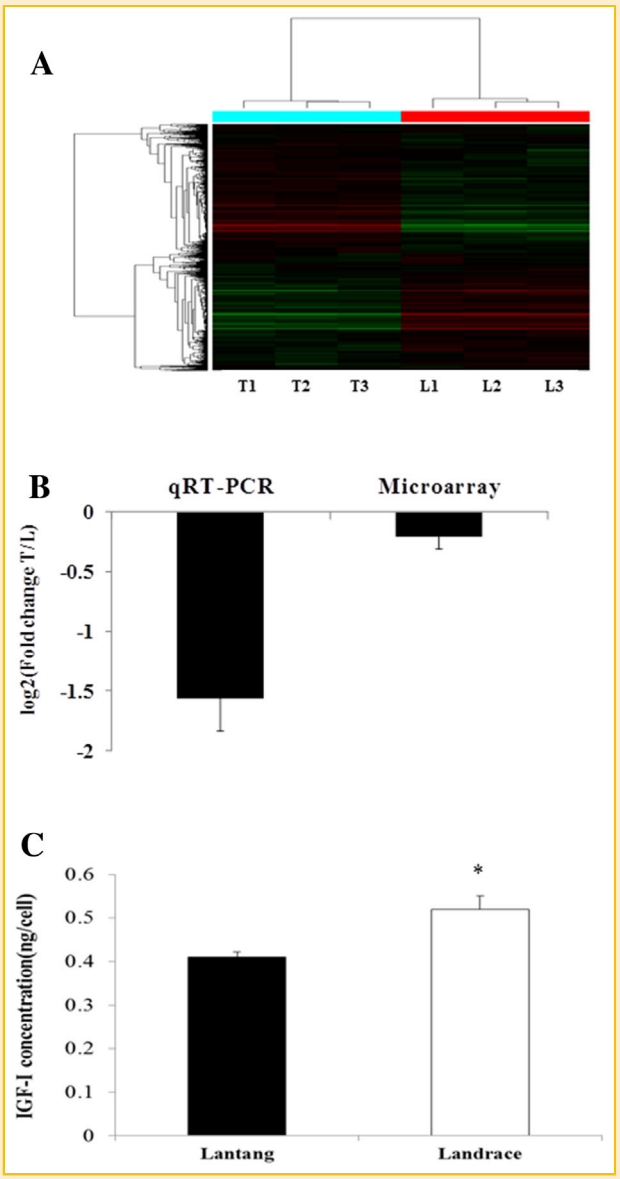

Fig 1. Difference in IGF-I gene expression and concentration in Lantang and Landrace satellite cells (SCs).SCs were cultured in DMEM/F12 medium containing 10% FBS. Cell culture medium was collected at 72 h after seeding. (A) Cluster analysis of differentially expressed genes between Lantang (T) and Landrace (L) SCs. Hierarchical clustering based on the median center-adjusted and normalized data. The red, green and black colors represent high, low, and absent expression levels, respectively, ($n = 3$). Fold change ≥ 1.5 and $P < 0.05$. (B) qRT-PCR validation of the microarray data on IGF-I gene expression ($n = 12$). The numbers here represent the fold change of IGF-1 gene expression in Lantang (T) versus Landrace (L). (C) IGF-I concentration in Lantang and Landrace SCs. IGF-I concentration in the medium was measured by radioimmunoassay ($n = 12$). Values are expressed as mean $\pm$ SEM. *Indicates a significant difference ($P < 0.05$).

EFFECTS OF LOW-AND HIGH-DOSE IGF-I SUPPLEMENTATION ON LANTANG SCs

To further determine the specific function of IGF-I, we treated Lantang SCs with two different doses (10ng/mL, 100ng/mL) of IGF-I. At the low dose (10 ng/mL), IGF-I significantly increased the size of the Lantang SCs ($P < 0.05$), but it had no effect on cell number ($P > 0.05$) (Fig. 3). In addition, compared with control group (0 ng/mL IGF-I), the mRNA and protein levels of Akt and S6K were found to be up-regulated ($P < 0.05$) at the low (10 ng/mL) dose of IGF-I treatments (Fig. 4).

In comparison, the high-dose (100 ng/mL) IGF-I supplementation resulted in an increase in both cell size and number (Fig. 3). Moreover, almost key genes in the mTOR pathway that we tested were significantly overexpressed ($P < 0.05$) at the high (100 ng/mL) dose of IGF-I treatments (Fig. 4). In addition, the protein levels of Akt, mTOR, eIF4E, and S6K were found to be up-regulated ($P < 0.05$) (Fig. 4)

LOW-DOSE IGF-I AFFECTS CELL SIZE THROUGH AKT/S6K BYPASSING mTOR

To elucidate the signaling mechanisms responsible for regulating cell size under low-dose IGF-I, we targeted Akt and S6K with two specific pharmacological inhibitors, MK2206 and PF4708671, respectively. We first showed that no significant differences in cell size were found at any time points between 24 and 60 h, whereas a significantly greater cell size ($P < 0.05$) was seen at 72 h in Lantang SCs that were treated with 10 ng/mL IGF-I (T10) than in untreated cells (T0) (Fig. 5A and 5B). There was no significance difference in cell number at any time points between the two groups (Fig. 5C). Therefore, we decided to add the inhibitors in T10 group at 60 h after seeding. After 12 h of drug treatment, both MK2206 and PF4708671 significantly reduced cell size ($P < 0.05$), as shown by HE staining and flow cytometry (Fig. 6A and 6B). In contrast to PF4708671, MK2206 reduced cell number in addition to cell size (Fig. 6C). To confirm whether the decrease in cell number could be due to cell death, we also analyzed the cell apoptosis by annexin V-FITC/PI staining and flow cytometry, and found that there was no significant difference ($P > 0.05$) in cell apoptosis among the groups (data not shown).

To determine the mechanisms behind the effects of the inhibitors on cell size in the presence of low-dose IGF-I, we assessed the levels of several key signaling proteins by western blot (Fig. 7). The levels of phosphorylated Akt (Ser473) and phosphorylated S6K (Thr389) were significantly higher in T10 than in T0 (Fig. 7A and Fig. 7D). MK2206 treatment had a great effect on the level of phosphorylated Akt (Ser473), S6K (Thr389), and rpS6 (Ser235/236) (Fig. 7A, 7D and 7E). PF4708671 reduced the level of phosphorylated S6K (Thr389) and its downstream target rpS6 (Ser235/236) (Fig. 7D and 7E). Neither MK2206 nor PF4708671 affected the level of p-mTOR (Ser2481) (Fig. 7B). What's more, IGF-I didn't affect the level of p-mTOR (Ser2448) and p-mTOR (Ser2481) (Fig. 7B and 7C). To determine whether Akt and S6K co-regulate cell size under low-dose IGF-I, MK2206, and PF4708671 were applied simultaneously. The combination of MK2206 and PF4708671 inhibited cell size to the same extent as the individual drug treatment (Fig. 7). The effects of the combination treatment on signaling proteins were almost the same as those of the Akt inhibition alone.

DISCUSSION

SCs were used in our investigation because their involvement in muscle growth appears to be linked to IGF-I. It has been shown that injury increases IGF-I synthesis by SCs in rodents, stimulating both

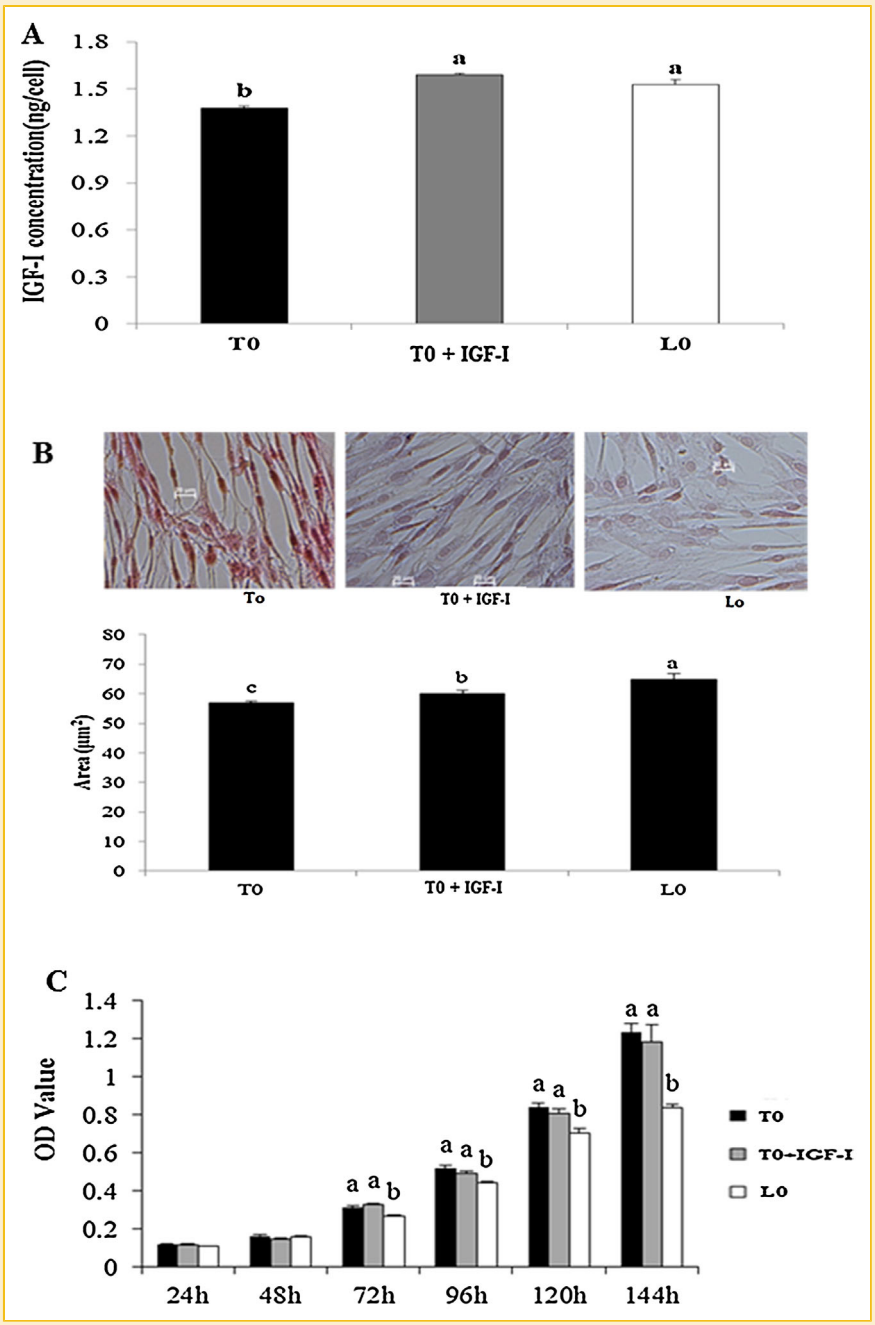

Fig. 2. Effects of IGF-I supplementation on satellite cells (SCs) size and cell viability. SCs were cultured in DMEM/F12 medium containing 10% FBS and with or without IGF-I. (A) IGF-I concentration in SCs culture medium at 72 h after seeding with the addition of exogenous IGF-I (n = 12). T0: Lantang SCs with DMEM/F12 (10% FBS); T0+IGF-I: Lantang SCs with DMEM/F12 (10%FBS) and 7 ng/mL IGF-I, which equalized IGF-I concentration in the culture medium of Lantang SCs and Landrace SCs at 72 h after seeding; L0: Landrace SCs with DMEM/F12 (10% FBS), as the control group. Measurement of cell size and viability with filling-in dose of IGF-I (7 ng/mL). (B) Cell size was measured via HE staining at 72 h after seeding (n = 6). (C) Cell viability was measured using the MTT assay at 24 h, 48 h, 72 h, 96 h, 120 h, and 144 h (n = 20). Values are expressed as mean ± SEM. Different superscript letters indicate statistically significant differences ($P < 0.05$).

cell proliferation and differentiation into myoblasts [Edwall et al., 1989]. Liu et al. [2008] have reported that the IGF-I gene is expressed at a lower level in the longissimus dorsi of Lantang pigs than in that of Landrace pigs at the age of 1 day. Our results were consistent with their in vivo data. Based on these data, IGF-I was considered to be different in two skeletal muscle satellite cell lines derived from two strains of pig. It suggested that these two cell lines were propose for further investigation of IGF-I. Moreover, IGF-I affected the two pig breeds SCs to a similar extent, therefore, there is no difference to select any of the two cell lines for further investigation.

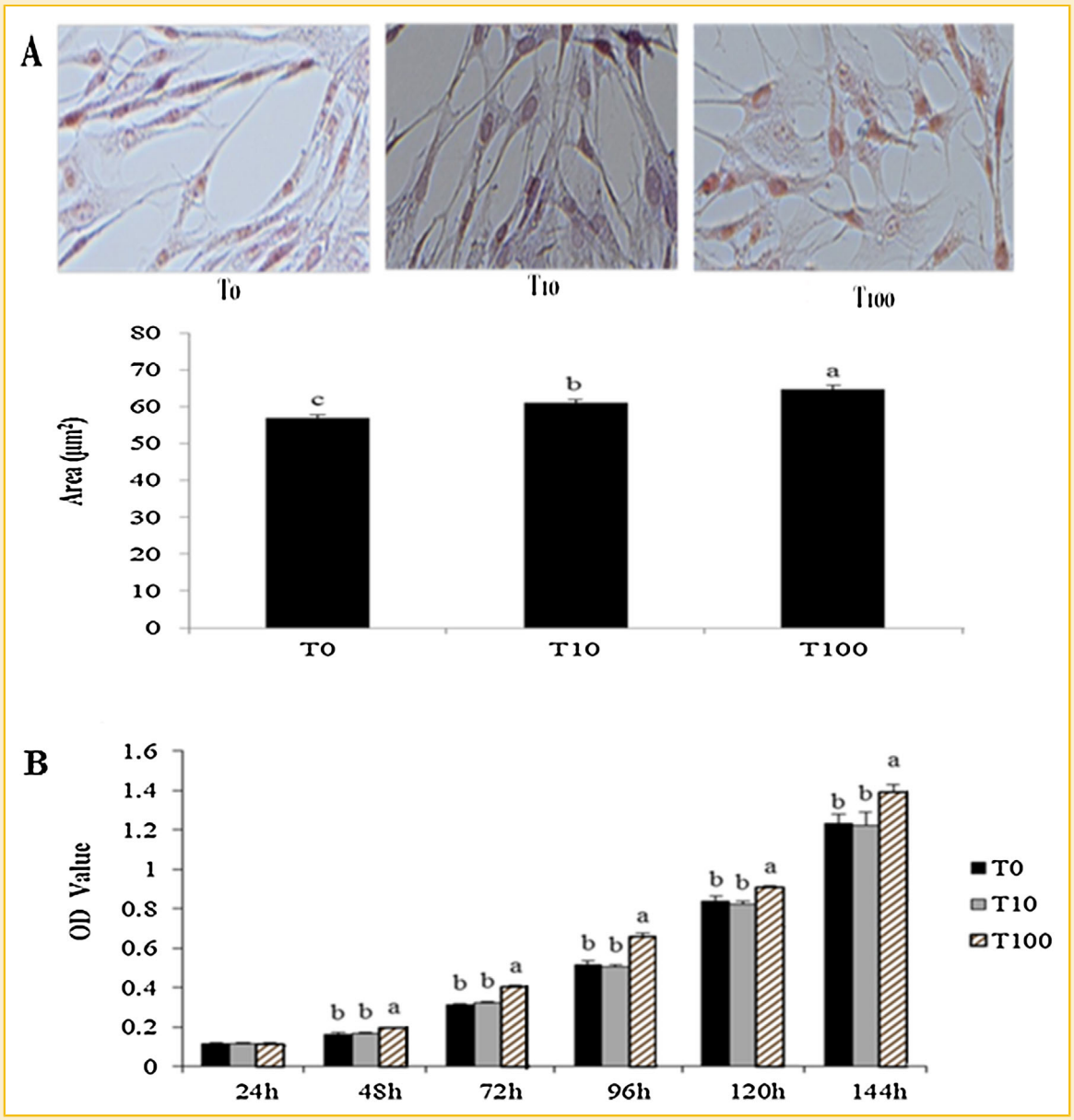

Fig. 3. Effects of low- and high-dose IGF-I treatments on Langtang satellite cells (SCs) size and viability. Cells were cultured in DMEM/F12 medium containing 10% FBS in the presence or absence of IGF-I. T0: Lantang SCs without IGF-I; T10: Lantang SCs with 10 ng/mL IGF-I; T100: Lantang SCs with 100 ng/mL IGF-I. (A) Cell size was measured via HE staining at 72 h after seeding ($n = 6$). (B) Cell viability was measured using the MTT assay at 24 h, 48 h, 72 h, 96 h, 120 h, and 144 h ($n = 20$). The results are representative of three separate experiments. Values are expressed as mean ± SEM. Different superscript letters indicate statistically significant differences ($P < 0.05$).

Interestingly, IGF-I affected cell phenotype, and more specifically, activation of the mTOR pathway depending on its concentration. Previous studies showed that IGF-I increases cell number and cell size mainly through activation of the PI3K/Akt/mTOR pathway [Spangenburg 2009; Fuentes et al., 2011; Sandri et al., 2013]. Our data from the high-dose IGF-I treatment are consistent with the findings of those studies. In contrast, we found that under low-dose IGF-I, there was no change in mTOR phosphorylation at Ser2448 and Ser2481. Low dose of IGF-I increased the protein level of Akt and S6K, suggesting that Akt/S6K may be involved in mediating the effect of IGF-I on cell size. As far as we know, this is the first report on the role of IGF-I in cell growth depending on its concentrations. Similar results have also been reported in another study showing that a 30 min incubation of quiescent human intestinal smooth muscle cells with IGF-I (0.1–100 nM) elicited a concentration-dependent increase in the levels of Akt and S6K phosphorylation [Kuemmerle, 2003]. Therefore, we conclude that IGF-I may stimulate cell growth via different pathways.

MK2206 is a recently developed allosteric inhibitor that has shown great promise in phase I clinical trials on patients with

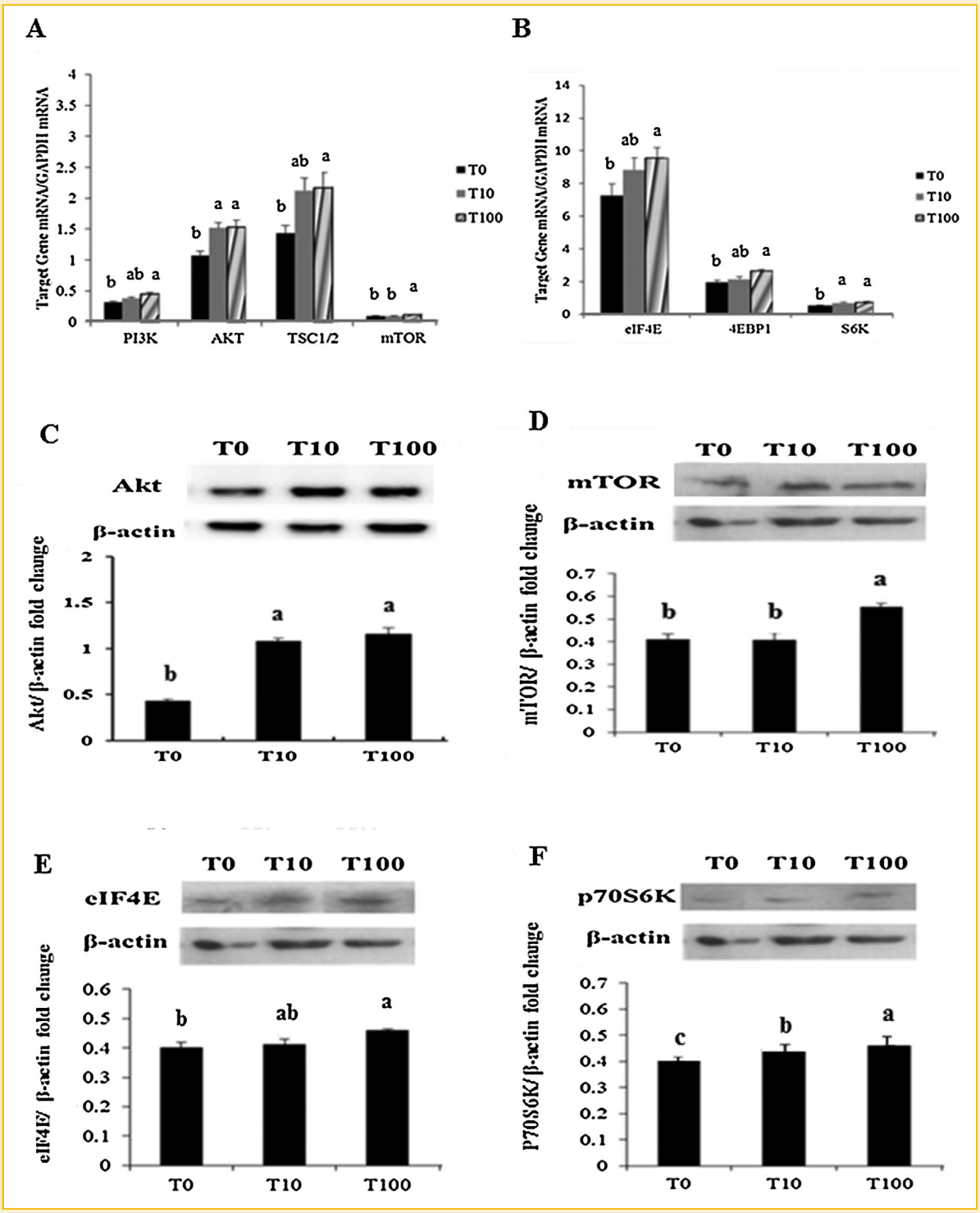

Fig. 4. Expression of key regulators of the mTOR pathway under low- and high-dose IGF-I treatments. Cells were cultured in DMEM/F12 medium containing 10% FBS in the presence or absence of IGF-I. T0: Lantang SCs without IGF-I; T10: Lantang SCs with 10 ng/mL IGF-I; T100: Lantang SCs with 100 ng/mL IGF-I. (A–B) Quantitative real-time RT-PCR analyses the genes mRNA abundance in satellite cells (SCs) that were treated with low- or high-dose IGF-I for 72 h after seeding ($n = 12$). GAPDH was used as an internal control gene. Western blot analysis of Akt (C), mTOR (D), eIF4E (E) and P70S6K (F) in SCs that were treated with low- or high-dose IGF-I for 72 h after seeding ($n = 4$). The β-actin was used as internal standard to normalization. Values are expressed as mean ± SEM. Different superscript letters indicate statistically significant differences ($P < 0.05$).

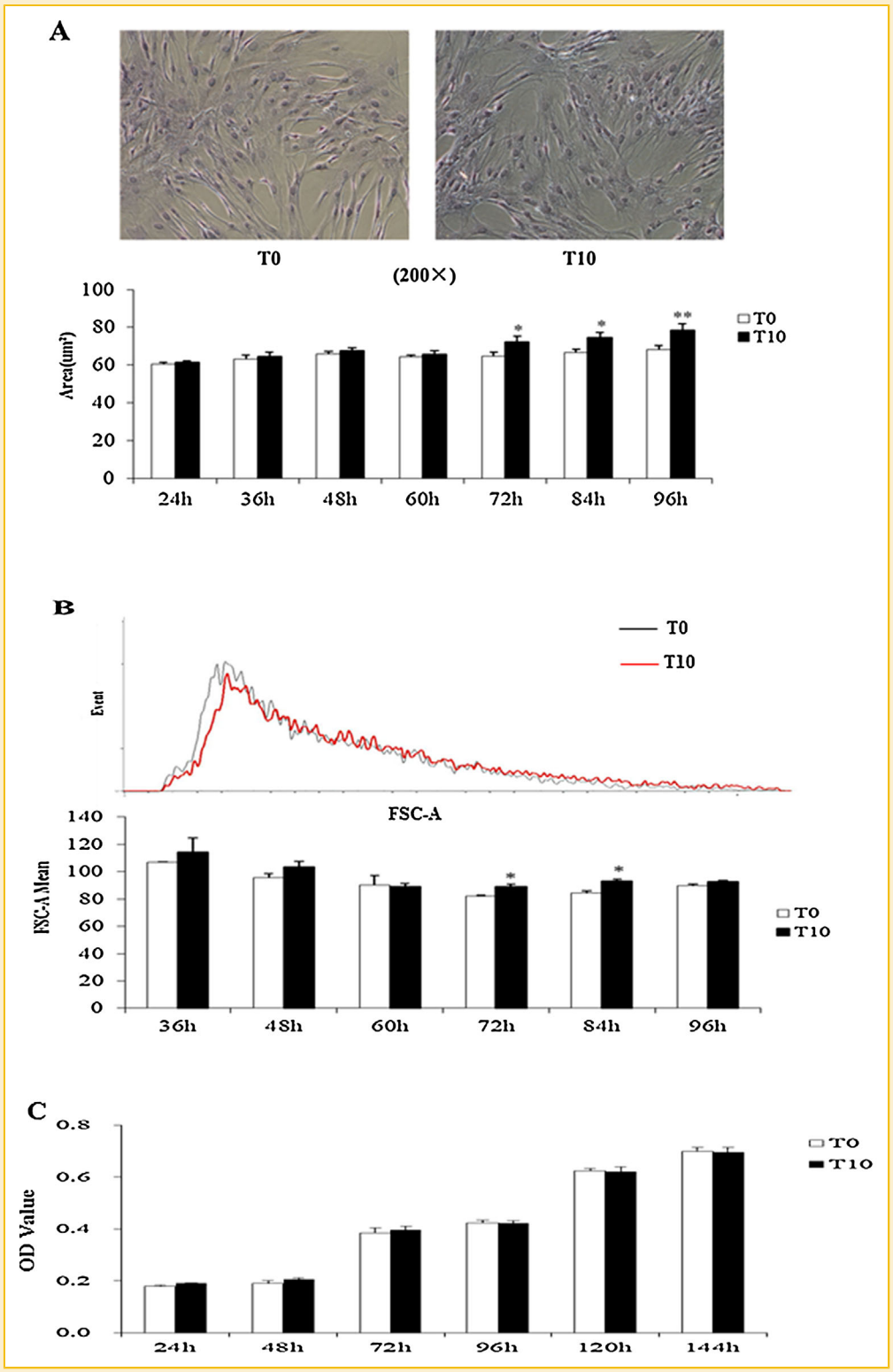

Fig. 5. Identification of the time at which satellite cells (SCs) size begins to increase under low-dose IGF-I treatment. Cells were cultured in DMEM/F12 medium containing 10% FBS with or without IGF-I. T0: Lantang SCs without IGF-I; T10: Lantang SCs with 10 ng/mL IGF-I. Cell size was measured by HE staining at 24 h, 36 h, 48 h, 60 h, 72 h, 84 h, and 96 h after seeding (A) and FCM analysis at 36 h, 48 h, 60 h, 72 h, 84 h, and 96 h after seeding (B) ($n = 6$). (C) Cell viability was measured using the MTT assay at 24 h, 48 h, 72 h, 96 h, 120 h, and 144 h ($n = 20$). Values are expressed as mean ± SEM. *Indicates a significant difference ($P < 0.05$).

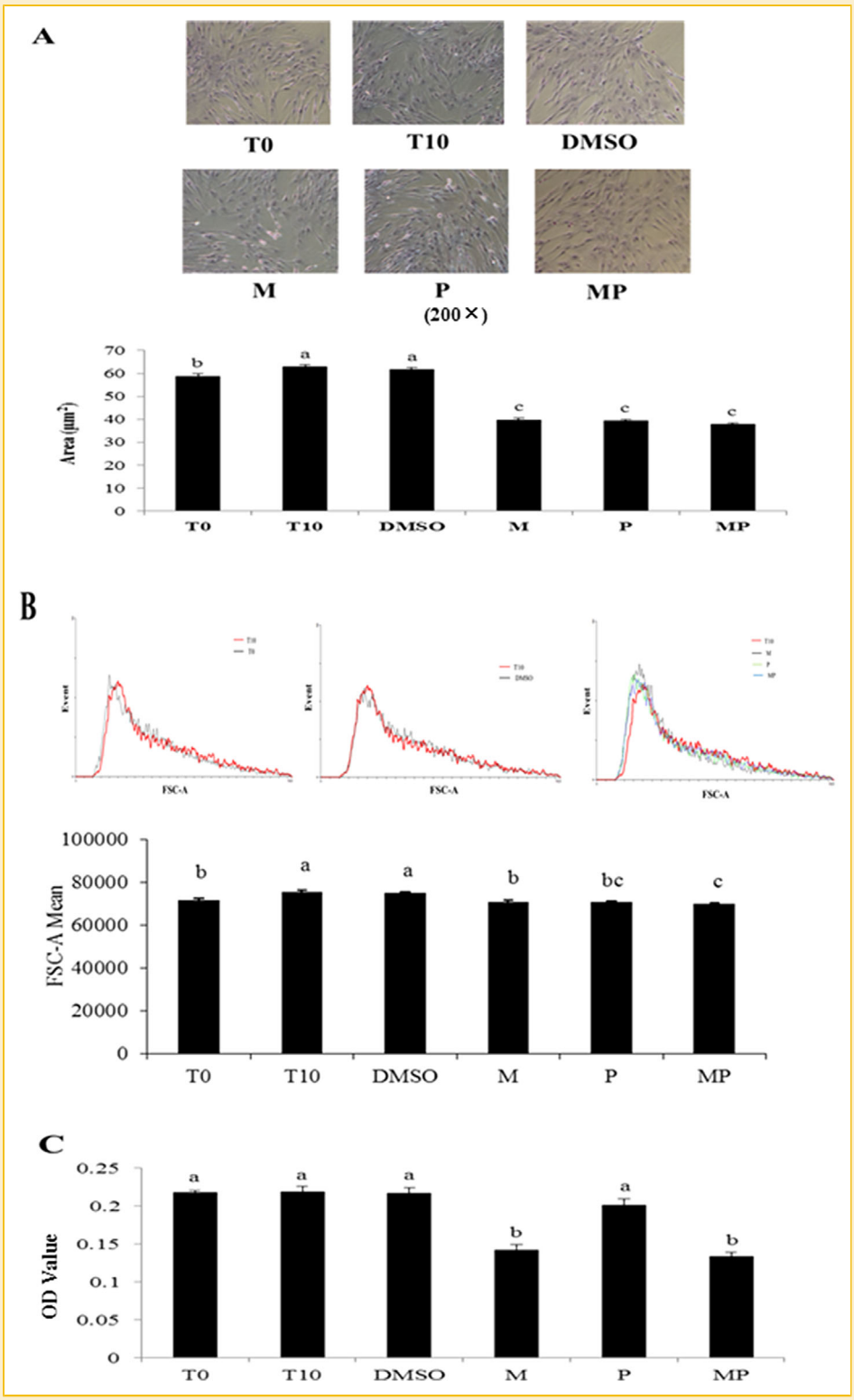

Fig. 6. Effects of Akt and S6K inhibitors on satellite cells (SCs) size and viability under low-dose IGF-I treatment. Cells were cultured in DMEM/F12 medium and 10% FBS with or without IGF-I and the inhibitors. The inhibitors were added at 60 h after seeding. T0: SCs in medium and FBS only; T10: SCs with 10 ng/mL IGF-I. DMSO: SCs with 10 ng/mL IGF-I and 0.1% DMSO, as the inhibitor control. M: SCs with 10 ng/mL IGF-I and 3.25 μmol/L MK2206. P: SCs with 10 ng/mL IGF-I and 8 μmol/L PF4708671. MP: SCs with 10 ng/mL IGF-I, 3.25 μmol/L MK2206, and 8 μmol/L PF4708671. Cell size was measured by HE staining (A) and FCM (B) at 72 h after seeding ($n = 6$). Cell viability was measured by MTT at 72 h after seeding (C) ($n = 15$). Values are expressed as mean ± SEM. Different superscript letters indicate statistically significant differences ($P < 0.05$).

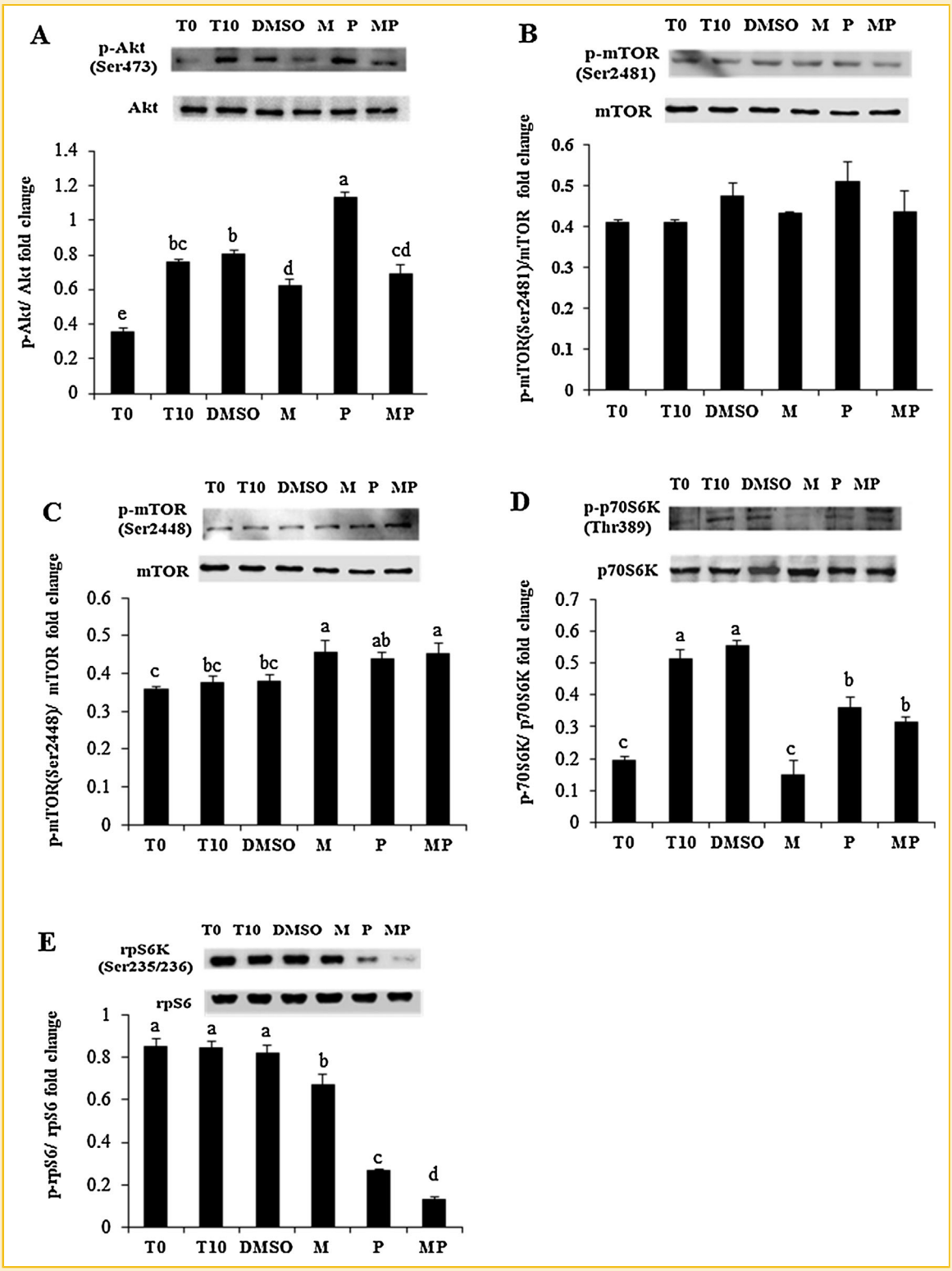

Fig. 7. Expression of mTOR pathway regulators under low level of IGF-I, Akt and S6K inhibitors treatment. Western blot analysis of the phosphorylation statue of mTOR signaling pathway in SCs at 72 h after seeding. T0: SCs in medium and FBS only; T10: SCs with 10 ng/mL IGF-I. DMSO: SCs with 10 ng/mL IGF-I and 0.1% DMSO, as the inhibitor control. M: SCs with 10 ng/mL IGF-I and 3.25 μmol/L MK2206. P: SCs with 10 ng/mL IGF-I and 8 μmol/L PF4708671. MP: SCs with 10 ng/mL IGF-I, 3.25 μmol/L MK2206, and 8 μmol/L PF4708671. Means presented the quantitation of the phosphorylation fold changes of Akt (A), mTOR (Ser2448, B), mTOR (Ser2481, C), S6K (D), rpS6 (E), respectively ($n = 4$). Values are expressed as mean ± SEM. Different superscript letters indicate statistically significant differences ($P < 0.05$).

advanced solid tumors. In our study, MK2206 treatment blocked the effect of low-dose IGF-I on cell size, suggesting that Akt participates in cell size regulation. Notably, MK2206 also decreased cell number at the same time, indicating that Akt affects both cell size and cell number. Indeed, modulation of Akt expression produces large cell size phenotypes [Gu et al., 2011]. In addition, MK2206 decreased the protein level of p-S6K and p-rpS6, suggesting that Akt may affect cell size through the S6K pathway. We further noted that low level of IGF-I did not affect the protein level of mTOR, p-mTOR (Ser2481 and Ser 2448), while MK2206 increased the protein level of p-mTOR (Ser2448). As far as we know no study has ever shown that MK2206 regulated the expression of p-mTOR (Ser2448). The mechanism for MK2206 affecting the protein level of p-mTOR (Ser2448) warrants further study.

PF-4708671 is the first S6K-specific inhibitor to be reported and is a useful tool for delineating S6K-specific roles downstream of mTOR [Pearce et al., 2010]. In this study, inhibition of S6K clearly reduced cell size but not cell number, suggesting that S6K may also participate in cell growth induction under low-dose IGF-I. The role of S6K on cell growth was first demonstrated with the finding that inactivation of S6K in D. melanogaster resulted in severe developmental delay and lethality with a marked reduction in body and organ size in surviving animals [Montagne et al., 1999]. Similar to what we observed with MK2206, PF4708671 did not affect the level of p-mTOR (Ser2481 and Ser2448), indicating that S6K may regulate cell size independently of mTOR. In contrast, MEFs and myoblasts that were isolated from S6K1$^{-/-}$ knockout mice displayed a reduced cell size relative to wild-type controls but a similar cell size relative to wild-type MEFs that were treated with catalytic inhibitors of mTOR [Ohanna et al., 2005; Dowling et al., 2010]. Previous study also revealed that S6K is a major downstream effector of mTORC1-driven cell growth [Dowling et al., 2010]. mTORC1 was shown to directly phosphorylate S6K1 at the HM site Thr389 to promote S6K1 activity [Burnett et al., 1998]. Under certain cellular conditions, S6K can be activated independently of the mTOR pathway. Phosphatidic acid (PA) was identified to directly interact with S6K and increase its activity in an mTORC1-independent manner through PLD2-mediated synthesis of PA [Lehman et al., 2007]. Liu et al. [2013] indicated that high-frequency muscle contraction increases the phosphorylation of S6K at Thr389 independently of mTOR. Among many known substrates of S6K, rpS6 has been shown to be directly involved in cell size regulation via its phosphorylation [Ruvinsky et al., 2005]. Interestingly, we noticed that even though PF4708671 blocked rpS6 phosphorylation, the low-dose IGF-I treatment did not increase the level of p-rpS6. It is important to note that S6K can promote cell growth independently of rpS6 phosphorylation, as suggested by the presence of normal levels of rpS6 phosphorylation in small S6K$^{-/-}$ myotubes [Olivier et al., 1988]. The identification of additional S6K substrates requires further research. One candidate substrate is SKAR, which is a novel regulator of cell growth downstream of S6K, and it has been shown that SKAR knockdown reduces cell size [Richardson et al., 2004]. It is worth noting that PF4708671 increases the level of p-Akt (Ser473). Previous studies indicated negative feedback loop from S6Ks to Akt [Um et al., 2006; Miyazaki et al., 2011]. Our data may appear to lend credence to the belief.

In this study, no synergistic effect of MK2206 and PF4708671 treatments on cell size was observed. Based on the data, Akt and S6K involve in the process that low-dose IGF-I enlargers cell size, while Akt may be the upstream of S6K via directly or indirectly ways.

CONCLUSIONS

In conclusion, our results suggest that IGF-I may stimulate the enlargement of cell size through Akt/S6K-dependent pathways. To the best of our knowledge, this is the first report showing that low-dose (10 ng/mL) IGF-I treatment increases cell size through Akt/S6K-dependent pathways. Therefore, this study highlights the significance of cellular IGF-I concentration in cell growth regulation and provides a new perspective on the regulation of cell growth via IGF-I/Akt/S6K signaling pathway. The model might make an excellent animal model for human SCs study.

ACKNOWLEDGMENTS

This work was jointly supported by the National Basic Research Program of China (2012CB124704), the National 948 Program of China (2011-G35), and the Science and Technology Planning Project of Guangzhou, Guangdong Province, China (201300000035).

REFERENCES

Barton ER, DeMeo J, Lei HQ. 2010. The insulin-like growth factor (IGF)-I E-peptides are required for isoform-specific gene expression and muscle hypertrophy after local IGF-I production. J Appl Physiol 108:1069–1076.

Burnett PE, Barrow RK, Cohen NA, Snyder SH, Sabatini DM. 1998. RAFT1 phosphorylation of the translational regulators p70 S6 kinase and 4E- BP1. Proc Natl Acad Sci U S A 95:1432–1437.

Cheng LY, Bailey AP, Leevers SJ, Ragan TJ, Driscoll PC, Gould AP. 2011. Anaplastic lymphoma kinase spares organ growth during nutrient restriction in drosophila. Cell 146:435–447.

Condorelli G, Drusco A, Stassi G, Bellacosa A, Roncarati R, Iaccarino G, Russo MA, Gu Y, Dalton N, Chung C, Latronico MV, Napoli C, Sadoshima J, Croce CM, Ross J, Jr. 2002. Akt induces enhanced myocardial contractility and cell size in vivo in transgenic mice. Proc Natl Acad Sci U S A 106:12333–12338.

Dowling RJ, Topisirovic I, Alain T, Bidinosti M, Fonseca BD, Petroulakis E, Wang X, Larsson O, Selvaraj A, Liu Y, Kozma SC, Thomas G, Sonenberg N. 2010. MTORC1-mediated cell proliferation, but not cell growth, controlled by the 4E-BPs. Science 328:1172–1176.

Duan CM, Ren HX, Gao S. 2010. Insulin-like growth factors (IGFs), IGF receptors, and IGF-binding proteins: Roles in skeletal muscle growth and differentiation. Gen Comp Endocrinol 167:344–351.

Edwall D, Schalling M, Jennische E, Norstedt G. 1989. Induction of insulin-like growth factor I messenger ribonucleic acid during regeneration of rat skeletal muscle. Endocrinology 124:820–825.

Fuentes EN, Björnsson BT, Valdés JA, Einarsdottir IE, Lorca B, Alvarez M, Molina A. 2011. IGF-I/PI3K/Akt and IGF-I/MAPK/ERK pathways in vivo in skeletal muscle are regulated by nutrition and contribute to somatic growth in the fine flounder. Am J Physiol Regul Integr and Comp Physiol 300: 1532–1542.

Ge XM, Zhang YF, Jiang HL. 2013. Signaling pathways mediating the effects of insulin-like growth factor-I in bovine muscle satellite cells. Mol Cell Endocrinol 372:23–29.

Gu YY, Lindner J, Kumar A, Yuan WP, Magnuson MA. 2011. Rictor/mTORC2 Is Essential for Maintaining a Balance Between beta-Cell Proliferation and Cell Size. Diabetes 60:827–837.

Hinnebusch AG. 2012. Translational Homeostasis via eIF4E and 4E-BP1. Mol Cell 46:717–719.

Hoeffer CA, Klann E. 2010. MTOR signaling: At the crossroads of plasticity, memory and disease. Trends Neurosci 33:67–75.

Jaafar R, De Larichaudy J, Chanon S, Euthine V, Durand C, Naro F, Bertolino P, Vidal H, Lefai E, Némoz G. 2013. Phospholipase D regulates the size of skeletal muscle cells through the activation of mTOR signaling. Cell Commun and Signal 11:55.

Kuemmerle JF. 2003. IGF-I elicits growth of human intestinal smooth muscle cells by activation of PI3K, PDK-1, and p70S6 kinase. Am J Physiol Gastrointest and Liver Physiol 284:G411.

Lehman N, Ledford B, Di Fulvio M, Frondorf K, McPhail LC, Gomez-Cambronero J. 2007. Phospholipase D2-derived phosphatidic acid binds to and activates ribosomal p70 S6 kinase independently of mTOR. FASEB J 21:1075–1087.

Liu DW, Zhao YX, Ren GC, Zhang H, Wu ZF. 2008. Developmental differential of expression of IGF-I, IGF-IR and IGFBP3 genes in liver and muscle of Lantang and Landrace pigs. Acta Veterinaria et Zootechnica Sinica 39:866–872.

Liu Y, Vertommen D, Rider MH, Lai YC. 2013. Mammalian target of rapamycin-independent S6K1 and 4E-BP1 phosphorylation during contraction in rat skeletal muscle. Cell Signal 25:1877–1886.

Lloyd AC. 2013. The Regulation of Cell Size. Cell 154:1194–1205.

Ma Z, Zhang H, Yi L, Fan H, Lu C. 2012. Microarray analysis of the effect of *Streptococcus equi subsp. zooepidemicus* M-like protein in infecting porcine pulmonary alveolar macrophage. PLoS ONE 7(e):36452.

Miyazaki M, McCarthy JJ, Fedele MJ, Esser KA. 2011. Early activation of mTORC1 signalling in response to mechanical overload is independent of phosphoinositide 3-kinase/Akt signalling. J physiol 589:1831–1846.

Montagne J, Stewart MJ, Stocker H, Hafen E, Kozma SC, Thomas G. 1999. Drosophila S6 kinase: A regulator of cell size. Science 285:2126–2129.

Ohanna M, Sobering AK, Lapointe T, Lorenzo L, Praud C, Petroulakis E, Sonenberg N, Kelly PA, Sotiropoulos A, Pende M. 2005. Atrophy of S6K1(-/-) skeletal muscle cells reveals distinct mTOR effectors for cell cycle and size control. Nat Cell Biol 7:286–294.

Olivier AR, Ballou LM, Thomas G. 1988. Differential regulation of S6 phosphorylation by insulin and epidermal growth factor in Swiss mouse 3T3 cells: Insulin activation of type 1 phosphatase. Proc Natl Acad Sci U S A 85:4720–4724.

Pearce LR, Alton GR, Richter DT, Kath JC, Lingardo L, Chapman J, Hwang C, Alessi DR. 2010. Characterization of PF-4708671, a novel and highly specific inhibitor of p70 ribosomal S6 kinase (S6K1). Biochem J 431:245–255.

Richardson CJ, Bröenstrup M, Fingar DC, Jülich K, Ballif BA, Gygi S, Blenis J. 2004. SKAR is a specific target of S6 kinase 1 in cell growth control. Curr Biol 14:1540–1549.

Rosner M, Hofer K, Kubista M, Hengstschlager M. 2003. Cell size regulation by the human TSC tumor suppressor proteins depends on PI3K and FK BP38. Oncogene 22:4786–4798.

Ruvinsky I, Sharon N, Lerer T, Cohen H, Stolovich-Rain M, Nir T, Dor Y, Zisman P, Meyuhas O. 2005. Ribosomal protein S6 phosphorylation is a determinant of cell size and glucose homeostasis. Genes Dev 19:2199–2211.

Sandri M, Barberi L, Bijlsma AY, Blaauw B, Dyar KA, Milan G, Mammucari C, Meskers CG, Pallafacchina G, Paoli A, Pion D, Roceri M, Romanello V, Serrano AL, Toniolo L, Larsson L, Maier AB, Muñoz-Cánoves P, Musarò A, Pende M, Reggiani C, Rizzuto R, Schiaffino S. 2013. Signalling pathways regulating muscle mass in ageing skeletal muscle. The role of the IGF1-Akt-mTOR-FoxO pathway. Biogerontology 14:303–323.

Song YH, Song JL, Delafontaine P, Godard MP. 2013. The therapeutic potential of IGF-I in skeletal muscle repair. Trends in Endocrinol Metab 24:310–319.

Spangenburg EE. 2009. Changes in muscle mass with mechanical load: Possible cellular mechanisms. Appl Physiol Nutr Metab 34:328–335.

Um SH, D′Alessio D, Thomas G. 2006. Nutrient overload, insulin resistance, and ribosomal protein S6 kinase 1, S6 K1. Cell Metab 3:393–402.

Wang XQ, Yang WJ, Yang Z, Shu G, Wang SB, Jiang QY, Yuan L, Wu TS. 2012. The differential proliferative ability of satellite cells in Lantang and Landrace pigs. PloS ONE 7:e32537.

Ye F, Mathur S, Liu M, Borst SE, Walter GA, Sweeney HL, Vandenborne K. 2013. Overexpression of IGF-1 attenuates skeletal muscle damage and accelerates muscle regeneration and functional recovery after disuse. Exp Physiol 98:1038–1052.

Zhang W, Shen X, Wan C, Zhao Q, Zhang L, Zhou Q, Deng L. 2012. Effects of insulin and insulin-like growth factor 1 on osteoblast proliferation and differentiation: Differential signalling via Akt and ERK. Cell Biochem Funct 30:297–302.